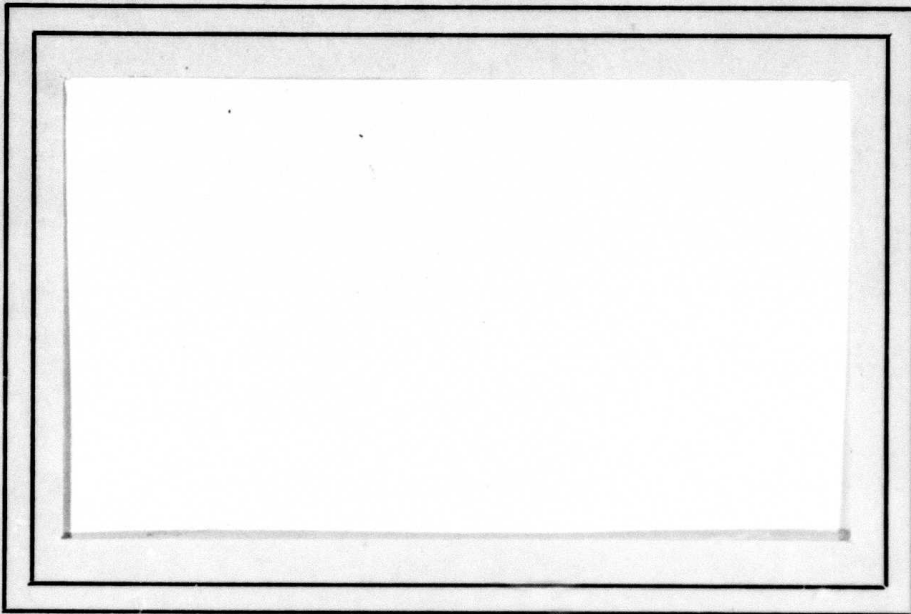


ADA 084291

①

LEVEL II



COMPUTER SCIENCE
TECHNICAL REPORT SERIES



UNIVERSITY OF MARYLAND
COLLEGE PARK, MARYLAND

20742

DISTRIBUTION STATEMENT A
Approved for public release
Distribution Unlimited

DTIC
ELECTE
MAY 19 1980
S E D

DDC FILE COPY

80 5 19 117

15 DAAG 53-76-C-0138
DARPA Order-3206

12 33

14 TR-789
DAAG-53-76C-0138

11 July 1979

6 FITTING MOSAIC MODELS
TO TEXTURES.

10 Narendra Ahuja
Azriel Rosenfeld

Computer Vision Laboratory
Computer Science Center
University of Maryland
College Park, MD 20742

9 Technical report

Accession For	
News	<input checked="" type="checkbox"/>
Doc TAB	<input type="checkbox"/>
Unannounced	<input type="checkbox"/>
Justification	<input type="checkbox"/>
By _____	
Date _____	
Distribution Codes	
Dist	and/or special
A	

ABSTRACT

Mosaic image models are defined by random geometric processes. Various properties of the patterns generated by such models can be predicted. Using these properties, we can fit the models to real images, and thus obtain insights into the structure of these images.

DISTRIBUTION STATEMENT A
Approved for public release
Distribution Unlimited

The support of the Defense Advanced Research Projects Agency and the U.S. Army Night Vision Laboratory under Contract DAAG-53-76C-0138 (DARPA Order 3206) is gratefully acknowledged, as is the help of Kathryn Riley in preparing this paper.

411 074

JOB

1. Introduction

In [1-5] various types of mosaic models for images were considered, and a number of properties of such models were derived. This paper reports some experiments on applying a set of mosaic models to several textures from the Brodatz album [6] and to some terrain textures.

Section 2 reviews the mosaic models and their properties. Section 3 discusses some issues concerning the modeling approach. Section 4 describes the experiments, and Section 5 presents some comments on the results.

2. Mosaic models

This section briefly reviews some planar geometrical processes that define the models, and presents the properties of components in binary images that are used in the experiments described in Section 4. For further details on the models, see [1-5,9].

We use the following notation:

p \equiv probability that a cell is colored black

λ \equiv intensity of the Poisson point process

d \equiv side length of a cell, or a square bomb

A_C \equiv expected component area

S_N \equiv expected number of cells per component when each cell has an expected number N of neighbors. Fig. 1 presents graphs of S_N as a function of p for $N = 3, 4$ and 6 .

P_C \equiv expected component perimeter.

2.1 Cell structure models

Cell structure mosaics are constructed in two steps:

- 1) Tessellate a planar region into cells. We will only consider tessellations composed of bounded convex polygons.
- 2) Independently assign one of m colors c_1, c_2, \dots, c_m to each cell according to a fixed set of probabilities

$$p_1, \dots, p_m; \sum_{i=1}^m p_i = 1$$

The set of colors may correspond to a set of values of any property, not necessarily gray level.

Cell structure models form a family whose members differ in the manner in which the plane is tessellated. We will describe some important members of this family, starting from the three regular tessellations and progressing towards random ones.

- a) Checkerboard model. In this model, the origin and orientation of the axes are chosen randomly, and the plane is tessellated into squares.

$$A_c = S_4 d^2$$

$$P_c = 4S_4 d(1-p)$$

- b) Hexagonal model. This is analogous to the checkerboard model, except that the plane is tessellated into regular hexagons.

$$A_c = 3\sqrt{3} S_6 d^2/2$$

$$P_c = 6S_6 d(1-p)$$

- c) Triangular model. This is analogous to the first two models, but based on tessellation into equilateral triangles.

$$A_C = \sqrt{3}S_3d^2/4$$

$$P_C = 3S_3d(1-p)$$

- d) Poisson line model. In this model, a Poisson process chooses points in the strip $0 \leq \theta < \pi, -\infty < \rho < \infty$. Each of these points defines a line of the form $x \cos \theta + y \sin \theta = \rho$, and these lines define a tessellation of the plane.

$$A_C = \frac{S_4}{\pi \lambda^2}$$

$$P_C = 2S_4(1-p)/\lambda$$

- e) Occupancy model. In this model, a Poisson process chooses points (called "nuclei") in the plane. Each nucleus defines a "Dirichlet cell" consisting of all the points in the plane that are nearer to it than to any other nucleus.

$$A_C = S_6/\lambda$$

$$P_C = 4S_6(1-p)/\sqrt{\lambda}$$

- f) Delaunay model. The Delaunay tessellation is obtained by joining all pairs of nuclei whose Dirichlet cells are adjacent.

$$A_C = S_3/2\lambda$$

$$P_C = \frac{32S_3(1-p)}{3\pi\sqrt{\lambda}}$$

2.2 Coverage models

Coverage or "bombing" models constitute the second class of mosaic models that we consider. A coverage mosaic is obtained by a random arrangement of a set of geometric figures ("bombs") in the plane.

We will now describe the class of binary coverage models. Consider a geometric figure in the plane and identify it by (i) the location of some distinguished point in the figure, e.g. its center of gravity, hereafter called the center of the figure; and (ii) the orientation of some distinguished line in the figure, e.g. its principal axis of inertia. Let a point process drop points on the plane and let each point represent the center of a figure. Let each figure have an orientation θ according to some distribution function $F(\theta)$. By this process any fixed region A is randomly partitioned into A_0 and $A_1 = A - A_0$, where A_1 consists of that part of A that is covered by the figures. By assigning two different colors to A_0 and A_1 , we get a binary coverage mosaic.

More generally, we can have more than one type of geometric figure, with the sizes of each class of figures governed by a certain probability distribution. These along with the nature of the point process and the choices of the probability distributions for color and orientation selection provide different ways of controlling the characteristics of the resulting patterns. For the experiments in this paper a single coverage

model was considered that uses upright squares of a fixed size and color having their centers distributed by a Poisson point process.

Figure 2 shows the expected total covered area, expected component area and expected component perimeter, all as functions of the expected number α of centers falling within a single square.

3. Model fitting

The model fitting process may consist of the following steps:

- a) Observe as many different features on the image as there are parameters defining the model. Use the observed feature values and their known dependence on the model parameters given in Section 2 to determine the parameter values.
- b) From the model thus specified, predict the values of the remaining known features. Compare these predictions with the observed values to estimate the model fit.

Alternatively, one may treat the entire set of known features simultaneously, and aim at obtaining values of the parameters such that the predicted features best fit the observed values. This avoids measuring the error only in terms of some of the features while fitting some others exactly.

Both of these approaches yield error vectors each consisting of the absolute errors in the fits of various features for a given model. The best model is the one that has the smallest error vector. The identification of the smallest vector, however, involves the following problems:

- 1) In the case when error in a single feature is being considered, the selection of the best model is trivial. In the general case, however, the individual terms in the vectors

must be normalized in order to obtain an overall error measure. Usually, normalization is carried out by expressing the error values in units of standard deviations. However, most known results for the mosaic models are for expected values, and not for distributions, or even standard deviations.

2) In combining normalized errors, the degree of orthogonality, or independence, among the corresponding features must be taken into account. Thus, if two features are correlated their errors should not be treated separately. For example, the area and perimeter of a convex shape completely determine its expected width [1]. Hence for textures with convex components the expected component width must not be considered if the component area and perimeter errors are used.

For these reasons, in this paper we use only one feature at a time to test the model fit.

The known characteristics of mosaic models include geometrical properties of components as well as correlation properties of pixels [1-5]. Since the latter are curves (functions of displacement) rather than single values, fitting them may involve a complicated process of error evaluation. Geometrical properties have therefore been used for model fitting in this paper.

4. Experimental results and discussion

Experiments were conducted on four textures from [6] (four samples of each) and on three terrain textures (three samples of each). Figure 3 (upper left) shows the samples of the seven textures. A foreground on a lighter background was identified in each of the images. An edge-based segmentation procedure that groups edges detected in the image into region boundaries by joining facing pairs of edge points [7] was used to convert the gray level images into binary images (Figure 3, upper right). Some of the small components may be due to noise. Also, some adjacent components may have been joined by noise. Without knowing the distribution of the component size, it is difficult to identify such components. To partially alleviate this problem, we have considered a set of binary images each derived from the original segmentation by deleting 8-connected components having areas smaller than a certain threshold. Figure 3 (bottom) shows the components having areas at least 10 and at least 13.

All six cell structure models and the square coverage model were considered. All of the cell structure models are completely specified in terms of the intensity of the point process and the color probability vector. In binary patterns there are only two colors. Therefore, the color probability vector has only one independent entry. The square coverage model is specified in terms of the intensity of the point process

and the side length of the square. Each model is therefore defined by two parameters. The values of a pair of features observed on each of the images are thus sufficient to evaluate the model parameters.

We now describe the features that we used in our experiments, and their estimation from the image data. Other features, such as component width, may also be used.

a) Black probability or total covered area

1) For cell structure models the fraction of the total number of cells that are colored black in a tessellation is an estimate of p . Since all the cells have the same expected area, the fraction of the total number of pixels in the image that are black is also an estimate of p .

2) For square coverage models the fraction of the area that is black is an estimate of the expected number α of centers that fall within a single square (Fig. 2).

b) Expected component area

In general, some of the image components will touch its borders and contribute only parts of their real areas to the image. Ignoring the lost area yields an underestimate of the expected component area. On the other hand if we consider a window sufficiently deep in the interior then although some of the components centered within the window do not completely lie within the window, there are others that have centers

outside the window but contribute parts of their areas within the window. Obviously the expected fraction of the area of a component centered inside the window that lies outside the window, or vice versa, is one-half [1]. Thus the total effective number of components that may be used for the computation of the expected component area is given by

Effective number of components within the window =

Total number of components completely within the window -
1/2 (total number of components touching the window borders)

and

Expected component area = $\frac{\text{Black area within the window}}{\text{Effective number of components within the window}}$

c) Expected component perimeter

As in the case of the area, the expected perimeter can be obtained as

Expected component perimeter = $\frac{\text{Total perimeter within the window}}{\text{Effective number of components within the window}}$

We estimated the perimeter from the digital borders of the components by weighting the steps connecting 4-neighbors by unity, and those connecting diagonal neighbors by $\sqrt{2}$. The computations were done in parallel at all the black pixels [8] instead of following the borders sequentially.

In our experiments (a) was always used as one of the two observations necessary for the parameter evaluation. Each of (b) and (c) was used once for the computation of the second

model parameter, and once for measuring the error in the model fit. Table 1 presents the errors in the predicted values of component perimeter and area, for samples of the seven textures of Fig. 3, when the component area and perimeter, respectively, are used for the model matching along with p . The errors in the fits of the square coverage model to all images are much higher than those of the other models and hence are not listed. The errors are listed for the threshold values of component size (10 and 13) which were found to most consistently provide minimum errors by the best-fitting models, within the range of size thresholds (0, 2, 4, 7, 10, 13, 16, 20) that were used. For each texture sample and for each threshold value, a six-tuple of errors is given corresponding to the absolute differences in the predicted and the observed values divided by the corresponding observed values. The six models used are checkerboard, hexagonal, triangular, Poisson line, occupancy, and Delaunay. The lowest errors are underlined, and the next lowest are usually underlined with dashes.

From the table we can see that for the sand and grass textures, the hexagonal and the occupancy models, respectively, provide the best fits. For sand, the hexagonal model has the minimum error for all samples and for both thresholds. For grass the choice between hexagonal and occupancy models is ambiguous at $T = 10$, but for $T = 13$ the occupancy model is

IMAGE	SAMPLE	ERROR PARAMETER	Component Size Threshold T											
			10						13					
			C	H	T	P	O	D	C	H	T	P	O	D
WOOL	1	Per	.13	<u>.00</u>	.20	<u>.11</u>	.13	.28	<u>.08</u>	<u>.06</u>	.15	.17	<u>.08</u>	.23
		Area	.07	<u>.00</u>	.12	<u>.05</u>	.07	.18	<u>.04</u>	<u>.03</u>	.08	.08	<u>.04</u>	.14
	2	Per	.14	.13	<u>.05</u>	.45	<u>.02</u>	<u>.05</u>	.21	.23	.11	.53	<u>.06</u>	<u>.00</u>
		Area	.06	.06	<u>.02</u>	.17	<u>.01</u>	.03	.09	.10	.05	.19	<u>.03</u>	<u>.00</u>
	3	Per	.06	<u>.01</u>	<u>.02</u>	.35	.14	.12	.09	.08	<u>.01</u>	.39	<u>.06</u>	.09
		Area	.03	<u>.00</u>	<u>.01</u>	.14	.08	.06	.04	.04	<u>.01</u>	.15	<u>.03</u>	.05
RAFFIA	1	Per	<u>.15</u>	.35	.31	.46	.43	<u>.18</u>	<u>.17</u>	.33	.33	.49	.42	<u>.20</u>
		Area	<u>.07</u>	.24	.13	.17	.33	<u>.08</u>	<u>.08</u>	.22	.13	.18	.32	<u>.09</u>
	2	Per	<u>.13</u>	.33	.25	.44	.42	<u>.12</u>	<u>.14</u>	.32	.26	.46	.41	<u>.14</u>
		Area	<u>.06</u>	.22	.10	.17	.31	<u>.06</u>	<u>.07</u>	.21	.11	.17	.30	<u>.06</u>
	3	Per	<u>.29</u>	<u>.19</u>	.49	.65	.30	.35	.32	<u>.17</u>	.52	.68	<u>.28</u>	.37
		Area	<u>.12</u>	<u>.11</u>	.18	.22	.19	.14	<u>.13</u>	<u>.10</u>	.19	.23	.18	.15
SAND	1	Per	.71	<u>.01</u>	.92	1.18	.14	.73	.75	<u>.01</u>	.96	1.23	.13	.77
		Area	.24	<u>.01</u>	.28	.32	.08	.24	.24	<u>.00</u>	.29	.33	.07	.25
	2	Per	.83	<u>.04</u>	1.08	1.33	.10	.88	.83	<u>.04</u>	1.08	1.33	.10	.88
		Area	.26	<u>.02</u>	.31	.34	.05	.27	.26	<u>.02</u>	.31	.34	.05	.27
	3	Per	.61	<u>.11</u>	.90	1.04	.23	.71	.62	<u>.10</u>	.92	1.06	.23	.73
		Area	.21	<u>.06</u>	.27	.30	.14	.24	.21	<u>.05</u>	.28	.30	.13	.24
GRASS	1	Per	.65	<u>.05</u>	.85	1.10	<u>.18</u>	.67	.89	<u>.12</u>	1.08	1.40	<u>.03</u>	.88
		Area	.22	<u>.03</u>	.26	.31	<u>.10</u>	.23	.27	<u>.06</u>	.31	.35	<u>.01</u>	.27
	2	Per	.87	<u>.18</u>	1.16	1.38	<u>.02</u>	.95	1.14	<u>.36</u>	1.26	1.72	<u>.17</u>	1.04
		Area	.27	<u>.08</u>	.32	.35	<u>.01</u>	.28	.32	<u>.14</u>	.33	.39	<u>.08</u>	.30
	3	Per	.58	<u>.01</u>	.61	1.01	<u>.15</u>	.45	.74	<u>.14</u>	.71	1.21	<u>.02</u>	.54
		Area	.20	<u>.01</u>	.21	.29	<u>.08</u>	.17	.24	<u>.06</u>	.23	.33	<u>.01</u>	.19

Table 1. Errors in fitting six models to samples of seven textures.

C = checkerboard, H = hexagonal, T = triangular,

P = Poisson line, O = occupancy, D = Delaunay.

For each sample, the row labelled "Per" or "Area" gives the error in component perimeter (area) when the predicted component area (perimeter) is matched to the observed area (perimeter).

IMAGE	SAMPLE	ERROR PARAMETER	Component Size Threshold T											
			10						13					
			C	H	T	P	O	D	C	H	T	P	O	D
MISSISSIPPIAN	1	Per	<u>.04</u>	.11	.11	.22	<u>.04</u>	.20	<u>.03</u>	.19	.05	.31	<u>.03</u>	.14
		Area	<u>.02</u>	.05	.06	.10	<u>.02</u>	.12	<u>.01</u>	.08	.03	.13	<u>.01</u>	.08
	2	Per	<u>.07</u>	.08	.14	.19	<u>.07</u>	.22	<u>.02</u>	.13	.10	.24	<u>.02</u>	.19
		Area	<u>.03</u>	.04	.08	.08	<u>.03</u>	.13	<u>.01</u>	.06	.05	.10	<u>.01</u>	.11
	3	Per	.10	.12	<u>.01</u>	.40	<u>.03</u>	.09	.18	.37	.09	.51	.18	<u>.01</u>
		Area	.05	.05	<u>.01</u>	.15	<u>.02</u>	.05	.08	.14	.04	.19	.08	<u>.01</u>
	4	Per	.33	.23	.13	.69	<u>.06</u>	<u>.02</u>	.44	.33	.37	.84	<u>.16</u>	.23
		Area	.13	.10	.06	.23	<u>.03</u>	<u>.01</u>	.17	.13	.15	.26	<u>.07</u>	.10
PENNSYLVANIAN	1	Per	.70	<u>.07</u>	.96	1.16	<u>.07</u>	.77	.83	<u>.15</u>	1.11	1.33	<u>.00</u>	.91
		Area	.23	<u>.03</u>	.29	.32	<u>.04</u>	.25	.26	<u>.07</u>	.31	.35	<u>.00</u>	.28
	2	Per	.49	<u>.07</u>	.52	.90	.19	.37	.54	<u>.04</u>	.57	.96	<u>.17</u>	.41
		Area	.18	<u>.04</u>	.19	.27	.11	.15	.19	<u>.02</u>	.20	.29	<u>.10</u>	.16
	3	Per	.35	<u>.14</u>	.43	.72	.26	.29	.45	<u>.09</u>	.48	.85	<u>.22</u>	.33
		Area	.14	<u>.08</u>	.16	.24	.16	.12	.17	<u>.05</u>	.18	.26	<u>.13</u>	.13
	4	Per	.85	<u>.16</u>	1.13	1.35	<u>.01</u>	.92	1.19	<u>.39</u>	1.32	1.79	<u>.20</u>	1.09
		Area	.26	<u>.07</u>	.32	.35	<u>.00</u>	.28	.32	<u>.15</u>	.34	.40	<u>.09</u>	.31
LOWER PENNSYLVANIAN	1	Per	.29	.17	.14	.64	<u>.01</u>	.03	.30	.19	.16	.66	<u>.03</u>	<u>.04</u>
		Area	.12	.08	.06	.22	<u>.01</u>	<u>.01</u>	.12	.08	.07	.22	<u>.01</u>	<u>.02</u>
	2	Per	.14	.07	<u>.05</u>	.45	.08	<u>.05</u>	.24	.22	.14	.57	.06	<u>.03</u>
		Area	.06	<u>.03</u>	<u>.03</u>	.17	.04	<u>.03</u>	.10	.10	.06	.20	.03	<u>.01</u>
	3	Per	.07	.24	<u>.01</u>	.37	.07	.11	.16	.34	.07	.48	.16	<u>.03</u>
		Area	.04	.10	<u>.00</u>	.14	.04	.06	.07	.14	.03	.18	.07	<u>.02</u>
	4	Per	.19	.11	.10	.51	.04	<u>.01</u>	.21	.20	.12	.54	.04	<u>.01</u>
		Area	.08	.05	.05	.19	.02	<u>.01</u>	.09	.09	.05	.19	.02	<u>.00</u>

Table 1, continued

consistently better. The checkerboard model fairly consistently describes the raffia texture at $T = 13$. Wool does not seem to fit any of our models well, although at $T = 13$ the occupancy model consistently results in errors that are second lowest.

Among the terrain textures the occupancy model gives the minimum errors for all but one of the Mississippian samples ($T = 13$). The Delaunay model provides a good fit to the Lower Pennsylvanian samples ($T = 13$). For the Pennsylvanian samples, the hexagonal model provides a fairly good fit to all but one sample at $T = 10$, but at $T = 13$ the choice is ambiguous between the hexagonal and occupancy models.

Thus in most cases, one model stands out as the best choice. Also, the errors in perimeter and area almost always support the same model. The consistency over the different samples is good, although in some cases, e.g. Mississippian, Pennsylvanian, and raffia, one sample appears to be significantly different from the rest and supports a different model, though the error corresponding to the model suggested by the other samples is generally not much higher.

It is interesting to note that the given set of models provides errors that vary over a wide range, i.e., the minimum to maximum error range in any six-tuple is usually large. This shows that the models do have significant differences that are

relevant in the context of the images that we have used. The choice of a given model, clearly, need not have any implications about the physical process that may have given rise to the image under consideration, i.e., this process need not be related in any way to the planar geometrical process that defines the model. In our experiments, for example, the models only characterize patterns by their area-perimeter relationships. Each model embodies one such relationship and the model chosen for a given image is that whose area-perimeter curve in the feature space lies closest to the point representing the observed values of these features.

Clearly, many other features could also be tried and the consistency of the models that they suggest could then be studied. Also the errors in Table 1 may be expressed in alternative ways, so that the significance of variations in error values over the samples, and from model to model, may be studied on a statistical basis.

References

1. N. Ahuja, Mosaic models for image analysis and synthesis, Ph.D. dissertation, Department of Computer Science, University of Maryland, College Park, Maryland, 1979.
2. N. Ahuja, Mosaic models for images, 1: geometric properties of components in cell structure mosaics, submitted for publication.
3. N. Ahuja, Mosaic models for images, 2: geometric properties of components in coverage mosaics, submitted for publication.
4. N. Ahuja, Mosaic models for images, 3: spatial correlation in mosaics, submitted for publication.
5. N. Ahuja and A. Rosenfeld, Mosaic models for textures, submitted for publication.
6. P. Brodatz, Textures: A Photographic Album for Artists and Designers, Dover, New York, 1966.
7. T. Hong, C. R. Dyer, and A. Rosenfeld, Texture primitive extraction using an edge-based approach, University of Maryland Computer Science Technical Report TR-763, May 1979.
8. P. V. Sankar and E. V. Krishnamurthy, On the compactness of subsets of digital pictures, University of Maryland Computer Science Technical Report TR-587, September 1977.
9. B. Schachter and N. Ahuja, Random pattern generation processes, Computer Graphics and Image Processing 10, 1979, 95-114.

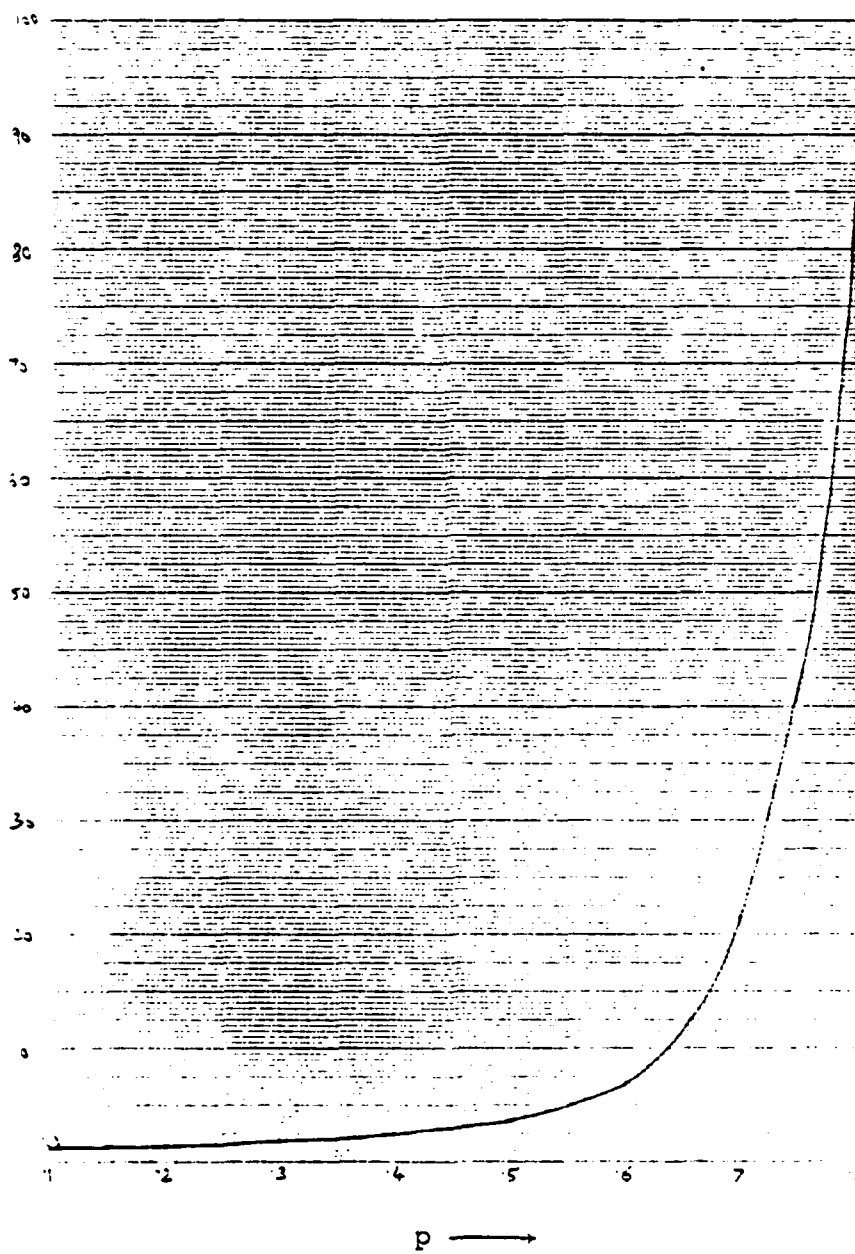


Figure 1a. S_3 as a function of p .

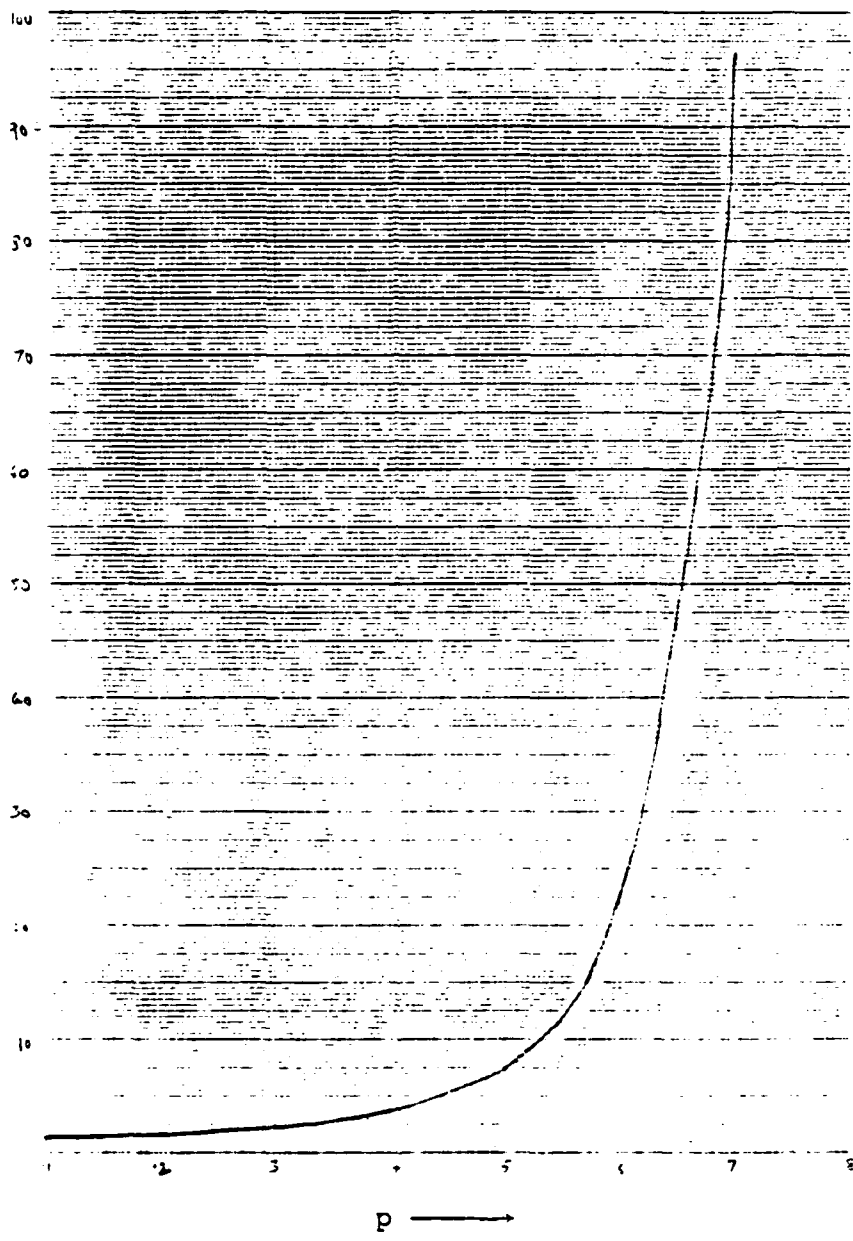


Figure 1b. S_4 as a function of p .

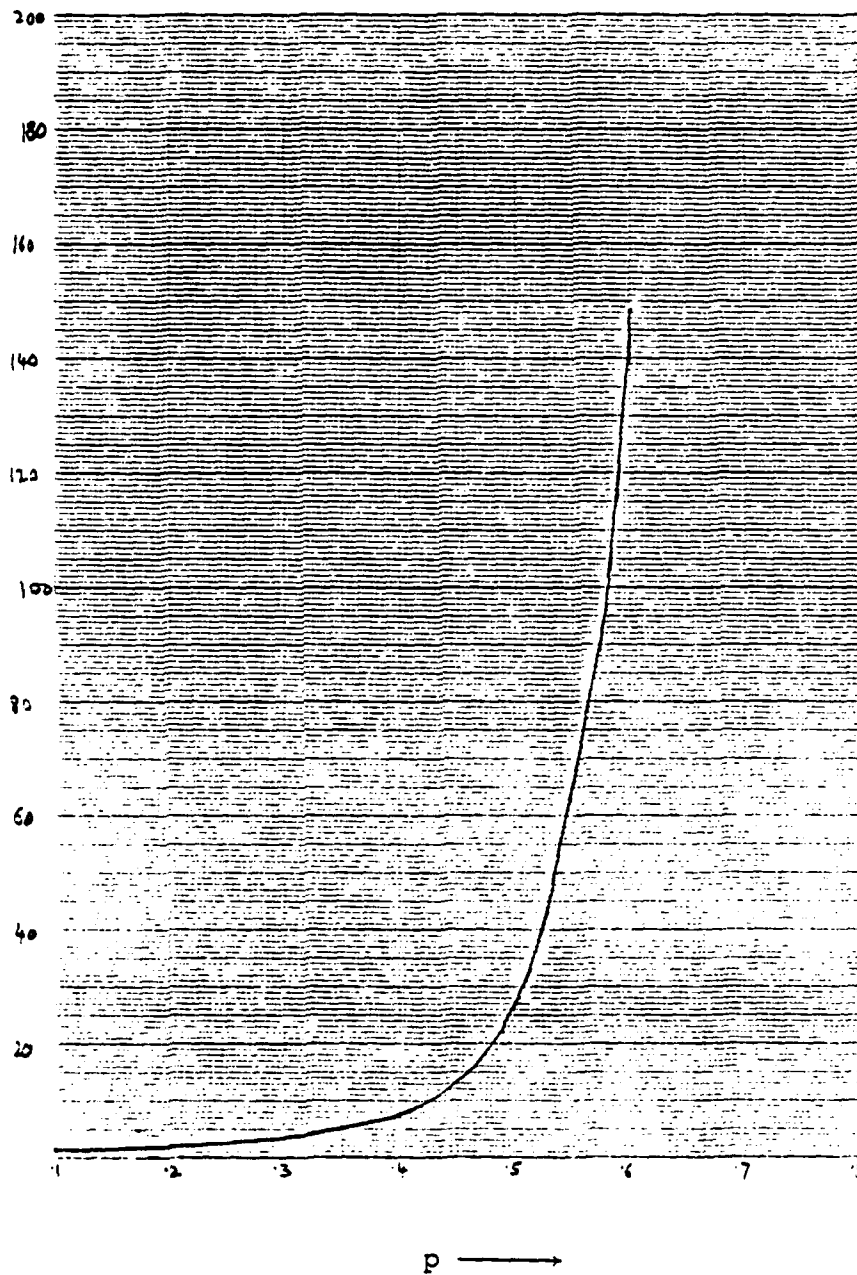


Figure 1c. S_6 as a function of p .

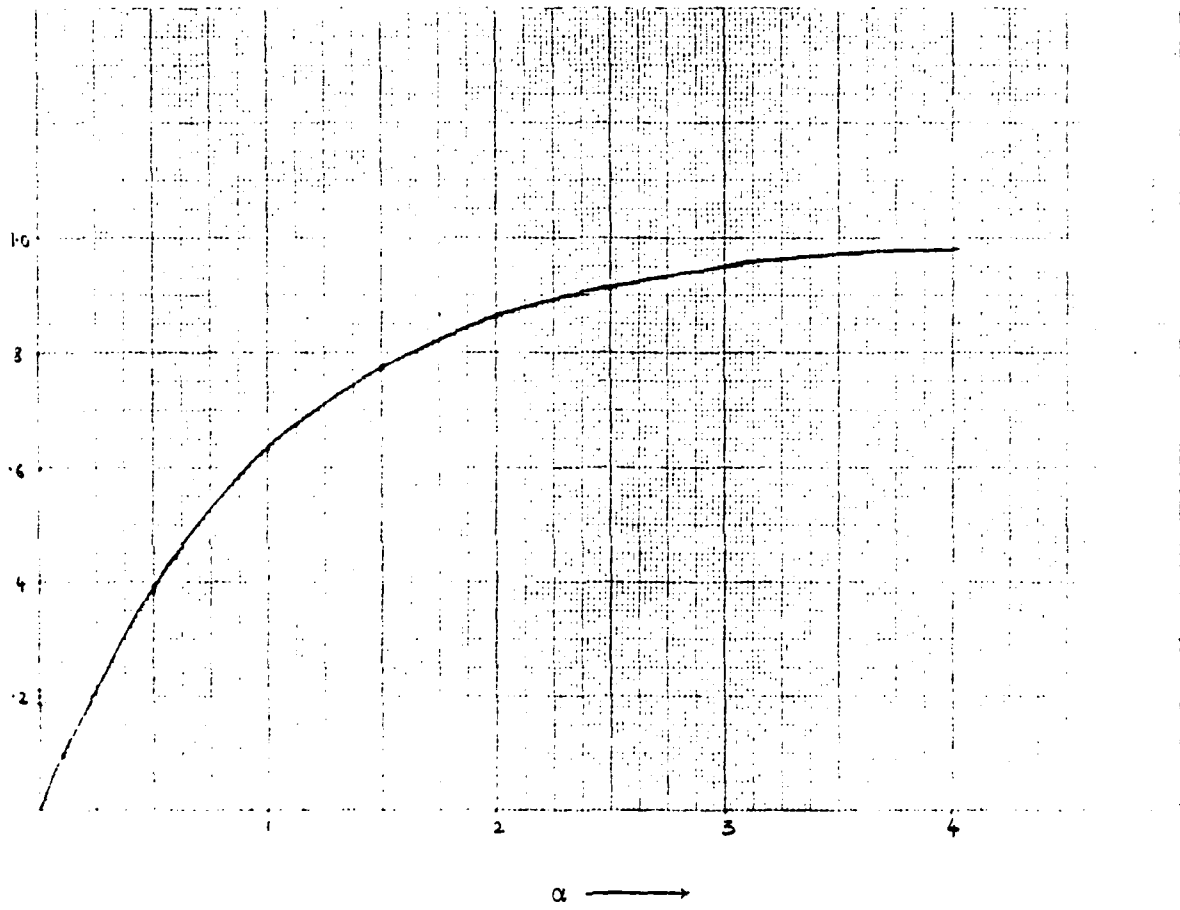


Figure 2a. Fraction of covered area as a function of α .

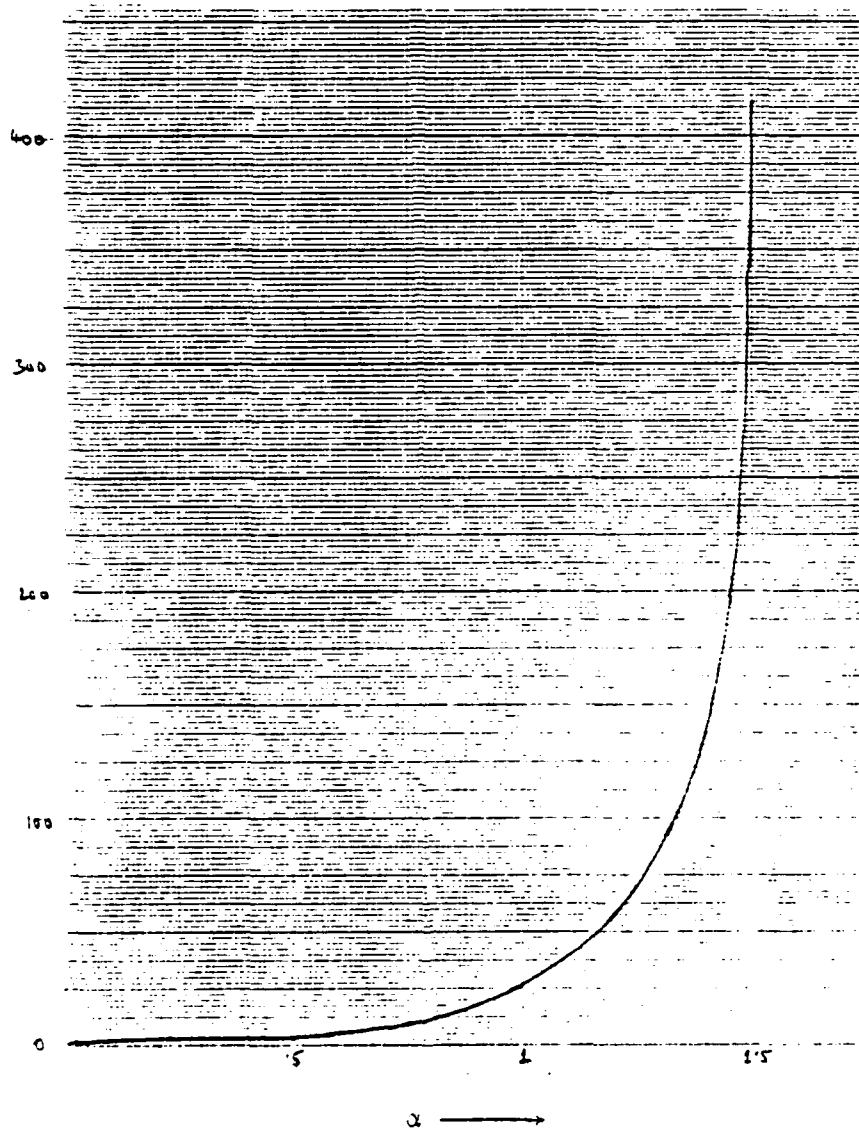


Figure 2b. Expected component area as a function of α .

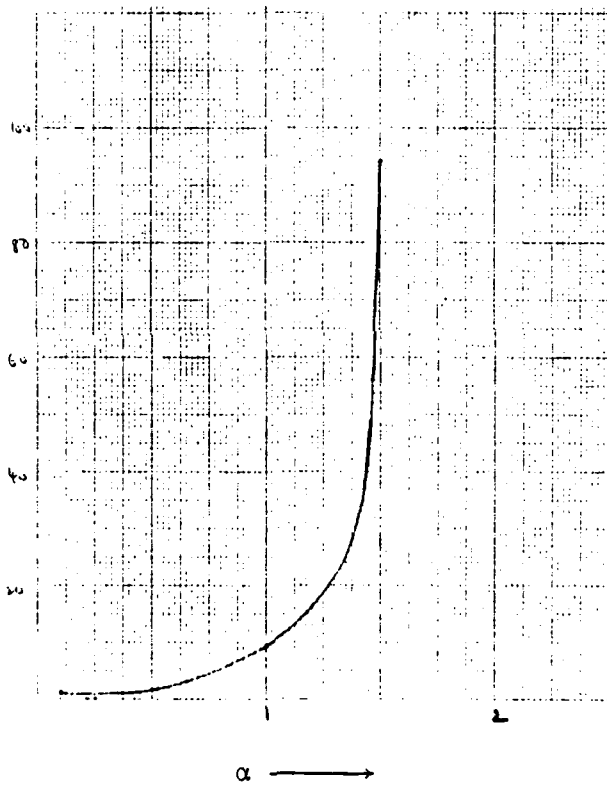
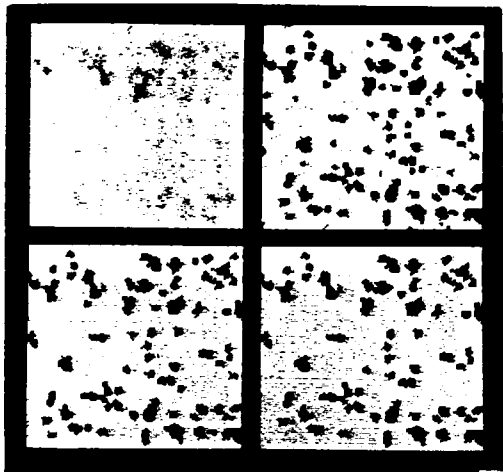
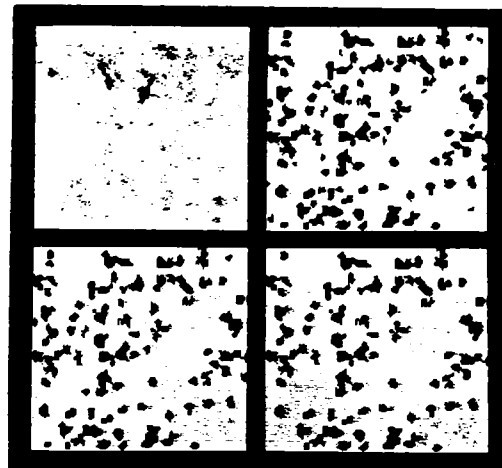


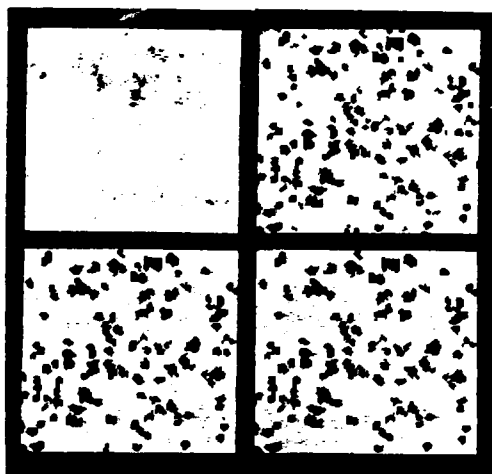
Figure 2c. Expected component perimeter as a function of α .



(1)



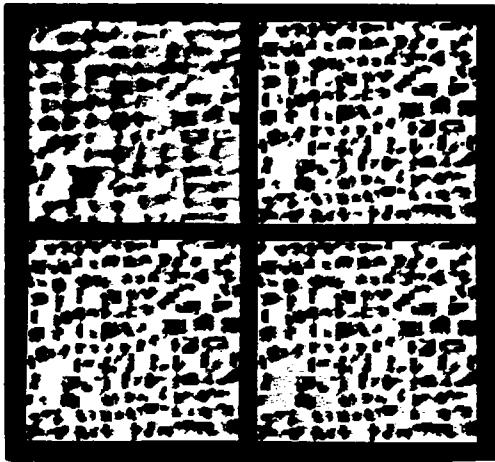
(2)



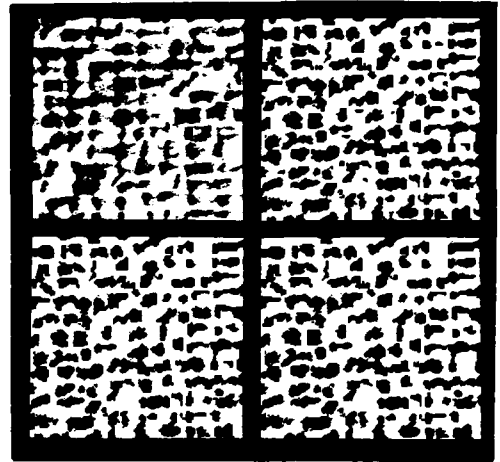
(3)

Figure 3. Texture samples (upper left), primitives (upper right), and primitives having areas ≥ 10 and ≥ 13 (lower left and right)

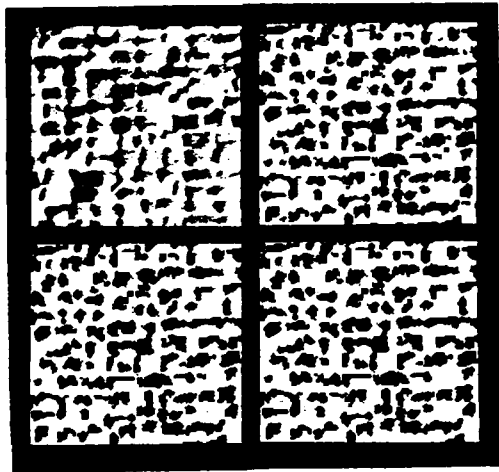
3a. Wool



(1)

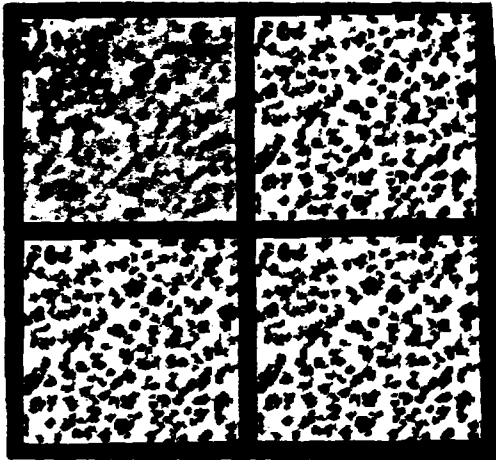


(2)

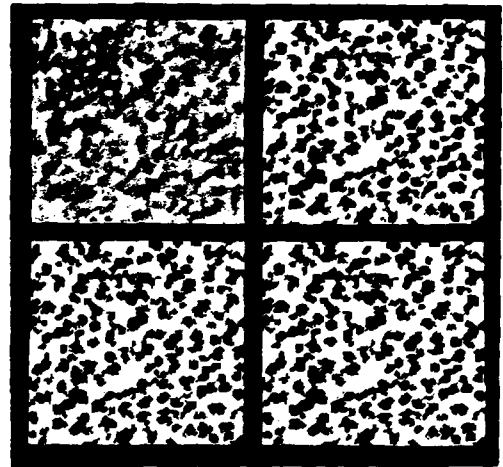


(3)

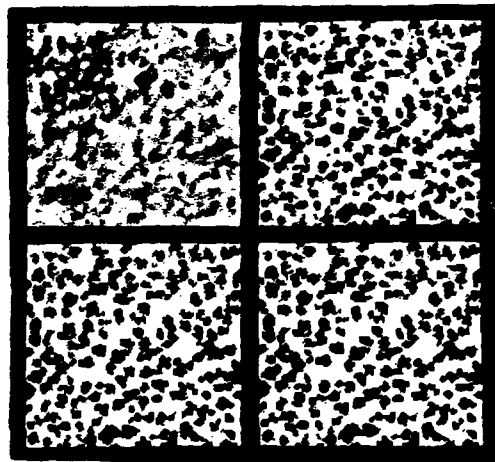
3b. Raffia



(1)

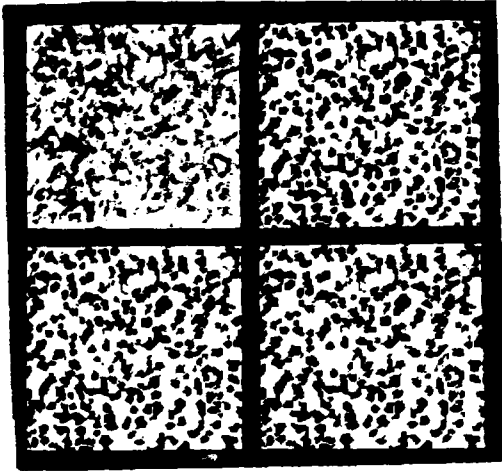


(2)

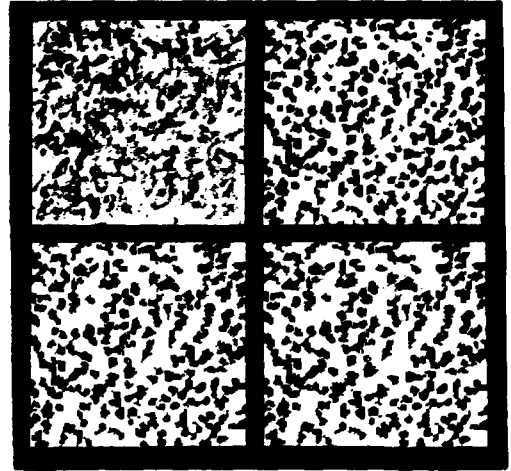


(3)

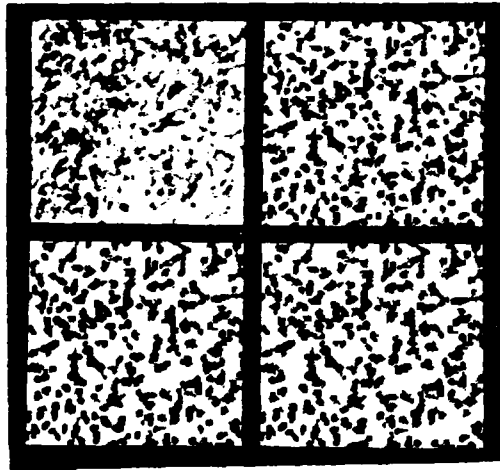
3c. Sand



(1)

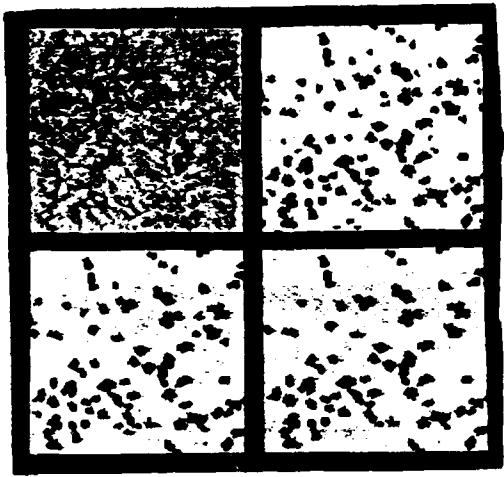


(2)

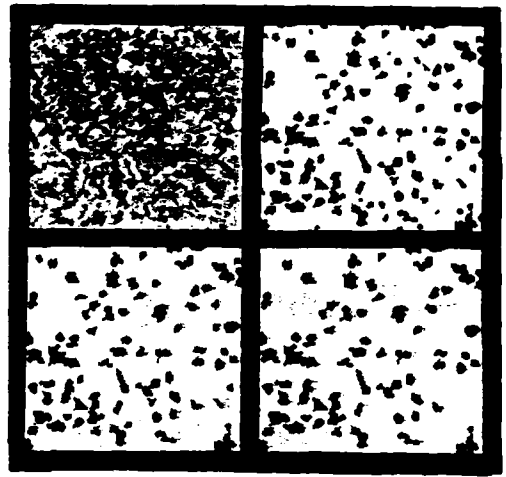


(3)

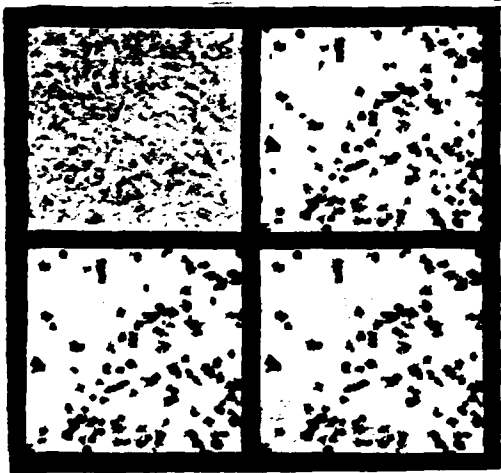
3d. Grass



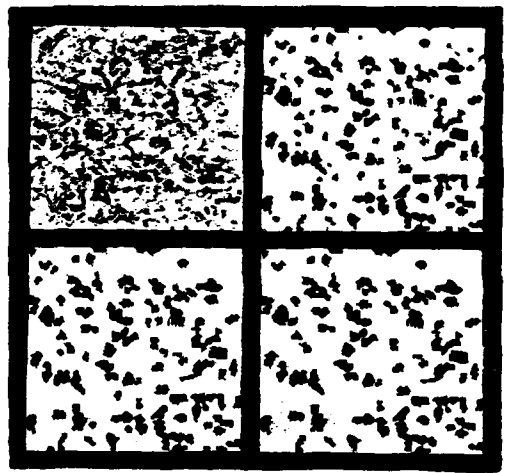
(1)



(2)

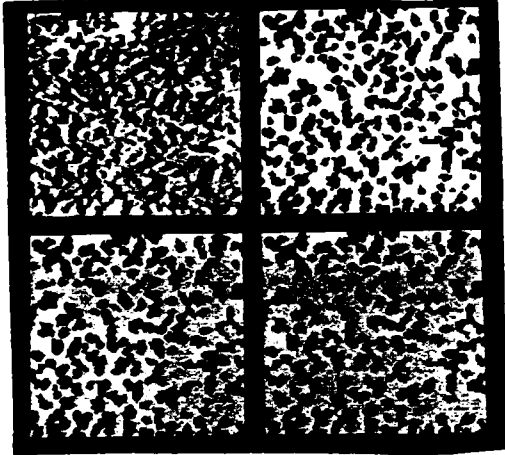


(3)

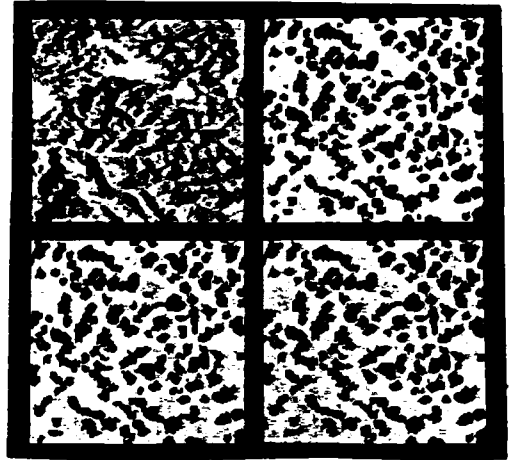


(4)

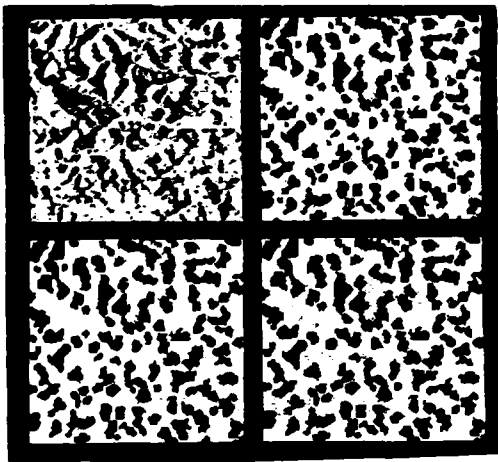
3e. Mississippian limestone and shale



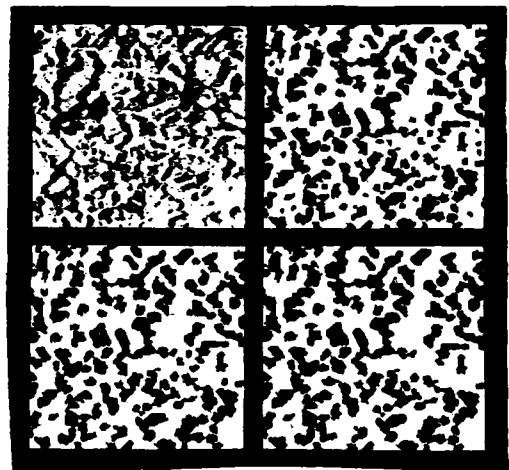
(1)



(2)

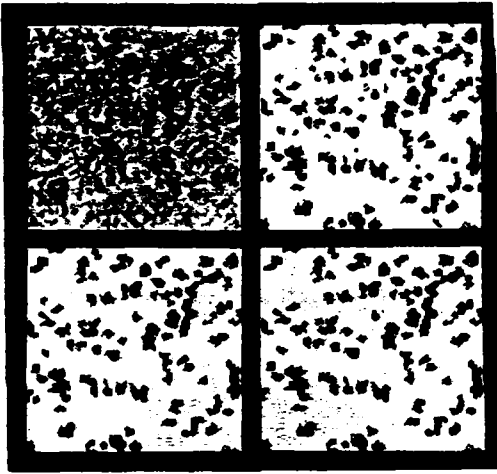


(3)

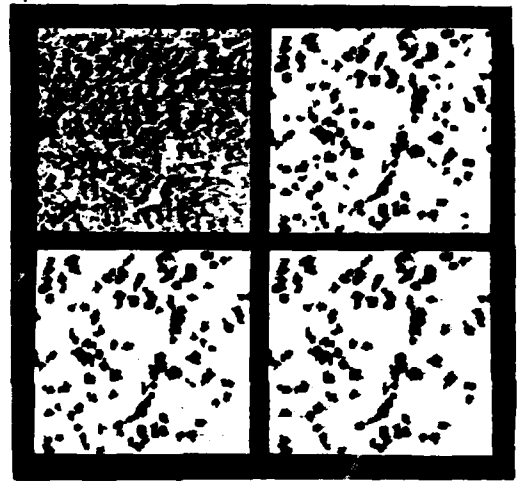


(4)

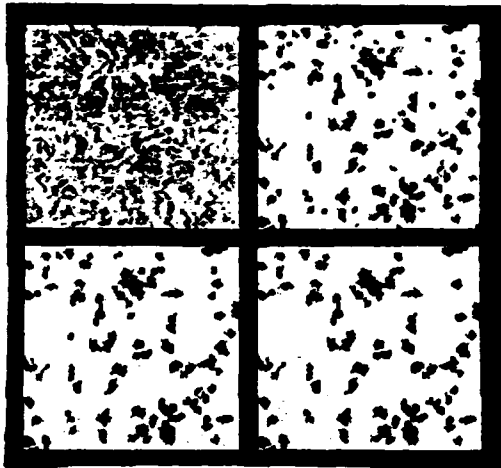
3f. Pennsylvanian sandstone and shale



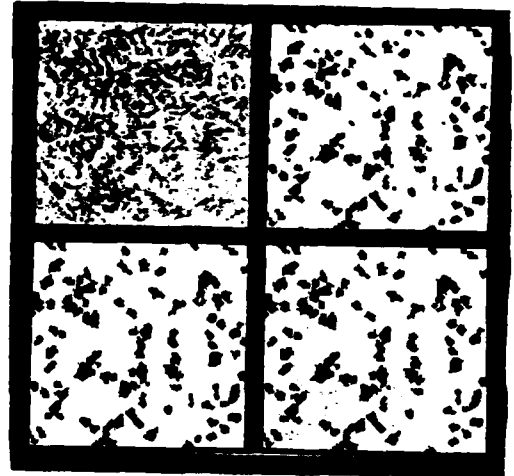
(1)



(2)



(3)



(4)

3g. Lower Pennsylvanian shale

Unclassified

SECURITY CLASSIFICATION OF THIS PAGE (When Data Entered)

REPORT DOCUMENTATION PAGE		READ INSTRUCTIONS BEFORE COMPLETING FORM
1. REPORT NUMBER	2. GOVT ACCESSION NO. AD-A084291	3. RECIPIENT'S CATALOG NUMBER
4. TITLE (and Subtitle) FITTING MOSAIC MODELS TO TEXTURES		5. TYPE OF REPORT & PERIOD COVERED Technical
		6. PERFORMING ORG. REPORT NUMBER TR-789
7. AUTHOR(s) Narendra Ahuja Azriel Rosenfeld		8. CONTRACT OR GRANT NUMBER(s) DAAG-53-76C-0138
9. PERFORMING ORGANIZATION NAME AND ADDRESS Computer Vision Laboratory Computer Science Center Univ. of Maryland, College Park MD 20742		10. PROGRAM ELEMENT, PROJECT, TASK AREA & WORK UNIT NUMBERS
11. CONTROLLING OFFICE NAME AND ADDRESS U.S. Army Night Vision Lab. Ft. Belvoir, VA 22060		12. REPORT DATE July 1979
		13. NUMBER OF PAGES 31
14. MONITORING AGENCY NAME & ADDRESS (if different from Controlling Office)		15. SECURITY CLASS. (of this report) Unclassified
		15a. DECLASSIFICATION/DOWNGRADING SCHEDULE
16. DISTRIBUTION STATEMENT (of this Report) Approved for public release; distribution unlimited.		
17. DISTRIBUTION STATEMENT (of the abstract entered in Block 20, if different from Report)		
18. SUPPLEMENTARY NOTES		
19. KEY WORDS (Continue on reverse side if necessary and identify by block number) Image processing Image models Random geometry Texture		
20. ABSTRACT (Continue on reverse side if necessary and identify by block number) Mosaic image models are defined by random geometric processes. Various properties of the patterns generated by such models can be predicted. Using these properties, we can fit the models to real images, and thus obtain insights into the structure of these images.		